ARTICLE
Journal of Cellular Biochemistry 113:1852–1867 (2012)

Journal of Cellular Biochemistry

The Inhibition of Hyaluronan Degradation Reduced Pro-Inflammatory Cytokines in Mouse Synovial Fibroblasts Subjected to Collagen-Induced Arthritis

Giuseppe M. Campo,* Angela Avenoso, Angela D'Ascola, Michele Scuruchi, Vera Prestipino, Giancarlo Nastasi, Alberto Calatroni, and Salvatore Campo

Department of Biochemical, Physiological and Nutritional Sciences, Section of Medical Chemistry, School of Medicine, University of Messina, Policlinico Universitario, 98125–Messina, Italy

ABSTRACT

Hyaluronan (HA) degradation produces small oligosaccharides that are able to increase pro-inflammatory cytokines in rheumatoid arthritis synovial fibroblasts (RASF) by activating both CD44 and the toll-like receptor 4 (TLR-4). CD44 and TLR-4 stimulation in turn activate the NF-kB that induces the production of pro-inflammatory cytokines. Degradation of HA occurs via two mechanisms: one exerted by reactive oxygen species (ROS) and one controlled by different enzymes in particular hyaluronidases (HYALs). We aimed to investigate the effects of inhibiting HA degradation (which prevents the formation of small HA fragments) on synovial fibroblasts obtained from normal DBA/J1 mice (NSF) and on synovial fibroblasts (RASF) obtained from mice subjected to collagen induced arthritis (CIA), both fibroblast types stimulated with tumor necrosis factor alpha (TNF-α). TNF-α stimulation produced high mRNA expression and the related protein production of CD44 and TLR-4 in both NSF and RASF, and activation of NF-kB was also found in all fibroblasts. TNF-α also up-regulated the inflammatory cytokines, interleukin-1beta (IL-1beta) and interleukin-6 (IL-6), and other pro-inflammatory mediators, such as matrix metalloprotease-13 (MMP-13), inducible nitric oxide synthase (iNOS), as well as HA levels and small HA fragment production. Treatment of RASF with antioxidants and specific HYAL1, HYAL2, and HYAL3 small interference RNA (siRNAs) significantly reduced TLR-4 and CD44 increase in the mRNA expression and the related protein synthesis, as well as the release of inflammatory mediators up-regulated by TNF-α. These data suggest that the inhibition of HA degradation during arthritis may contribute to reducing TLR-4 and CD44 activation and the inflammatory mediators response. J. Cell. Biochem. 113: 1852–1867, 2012. © 2012 Wiley Periodicals, Inc.

KEY WORDS: HYALURONAN; NF-kB; TOLL-LIKE RECEPTORS; CYTOKINES; CD44; COLLAGEN-INDUCED ARTHRITIS; SYNOVIAL FIBROBLASTS; HYALs; siRNA

Rheumatoid arthritis (RA) is characterized by synovial inflammation and destruction of joint cartilage and bone mediated by the continued synthesis of pro-inflammatory cytokines and tissue-destructive enzymes, such as matrix metalloproteinases (MMPs) and inducible nitric oxide synthase (iNOS), that are responsible for an increase in the detrimental free radical nitric oxide (NO) [Murphy and Nagase, 2008; Hueber et al., 2010; Nagy et al., 2010]. The synovial membrane is recognized as the primary pathogenic site in RA and has been particularly useful in the study of this destructive disease. Fibroblast-like synoviocytes (FLS), the major cellular constituent of synovial membranes, are the main contributors to the over-production of cartilage-degrading MMPs and reactive oxygen species (ROS) in arthritic joints [Cunnane et al., 2001; Filippin et al., 2008]. Among MMPs and ROS, MMP-13, the hydroxyl radical ($^{\bullet}OH$) and the superoxide anion ($^{\bullet}O_2^-$) seem to play a central role in bone and cartilage degradation [Hitchon and El-Gabalawy, 2004; Takaishi et al., 2008].

Cartilage erosion is also associated with an increased expression of inflammation mediators, for example, interleukin-1beta (IL-1β) and tumor necrosis factor alpha (TNF-α) [Gaston, 2008]. It is widely accepted that IL-1β and TNF-α are pro-inflammatory cytokines that are greatly involved in articular cartilage destruction as well as in the inflammatory response in arthritis.

The glycosaminoglycan hyaluronan (HA) is an important macromolecular component of synovial fluid.

During the response-to-injury, HA polymers are rapidly metabolized within the injured tissue [Tammi et al., 2008; Alaniz et al., 2009; Jackson, 2009; Sloane et al., 2010]. Local HA production

Grant sponsor: University of Messina, Italy.

*Correspondence to: Giuseppe M. Campo, PhD, Department of Biochemical, Physiological and Nutritional Sciences, School of Medicine, University of Messina, Policlinico Universitario, Torre Biologica, 5° piano, Via C. Valeria – 98125–Messina, Italy. E-mail: gcampo@unime.it

Manuscript Received: 31 October 2011; Manuscript Accepted: 5 January 2012
Accepted manuscript online in Wiley Online Library (wileyonlinelibrary.com): 10 January 2012
DOI 10.1002/jcb.24054 • © 2012 Wiley Periodicals, Inc.

and accumulation are increased as a result of elevated HA synthase expression in injured cells, and HA is then rapidly fragmented by extracellular hyaluronidases, ROS, and mechanical shearing [Stern, 2008; Monzon et al., 2010]. The functional effects of HA fragments and their clearance from the tissue undergoing repair are due to their binding to HA receptors such as CD44, RHAMM, and Toll-Like Receptors 2,4 (TLR-2,4) [Taylor et al., 2007; Campo et al., 2009; Campo et al., 2010ab; Stern et al., 2006]. Internalized low molecular weight HA is removed by the lysosome and further degraded into tetra and hexasaccharides mainly by the intracellular endoglycosidases, hyaluronidase 1 and 2 (HYAL1, HYAL2) [Veiseh and Turley, 2011]. The oligosaccharides produced by HYAL1 and HYAL2 are then further degraded by two lysosomal exoglycosidases, β-glucuronidase and β-N-acetyl hexosaminidase [Veiseh and Turley, 2011]. Small HA fragments have been found to elicit various pro-inflammatory responses such as CD44 and TLR-4 activation, thereby stimulating inflammation or increasing the inflammatory mechanism previously induced by other agents in different cell types. The separate stimulation of TLR4 and CD44 receptors may prime/amplify inflammatory response through NF-kB activation [Loniewski et al., 2007; Hutas et al., 2008].

The studies presented herein were conducted on normal mouse synovial fibroblasts (NSF) and rheumatoid arthritis synovial fibroblasts (RASF) stimulated with TNF-α. The aim was to examine the effects of pre-treatment with HYAL1, HYAL2, and HYAL3 small interference RNA (siRNAs) that inhibit HYAL1, HYAL2, and HYAL3 activity and also the effects of treatment with two antioxidants, i.e., uric acid (UA) plus superoxide dismutase (SOD), which are respectively the natural potent scavengers of the detrimental peroxynitrite ($ONOO^-$), formed through the action of elevated NO concentrations, and of superoxide anions (O_2^-).

MATERIALS AND METHODS

ANIMALS

Male mice DBA/J1 6–7 weeks old with a mean weight of 25–30 g were used in our study. Mice, purchased from Harlan (Correzzana, Italy), were maintained under climate-controlled conditions with a 12-h light/dark cycle. The animals were fed standard rodent chow and provided water ad libitum. The health status of the animal colony was monitored in accordance with Italian Veterinary Board guidelines. Mice were divided into two groups: (1) Control (n = 7), and (2) CIA (n = 10).

MATERIALS

Recombinant murine TNF-α obtained from E. coli source (cat. 315-01A) was purchased from Peprotech Inc. (Rocky Hill, NJA). Rabbit polyclonal antibodies against the CD44 receptor for western blot (cat. Ab41478) were supplied by Abcam Ltd (Cambridge, UK). Mouse HYAL1 siRNA (cat. sc-60823), HYAL2 siRNA (cat. sc-60825), HYAL3 siRNA (sc-60827), rabbit TLR-4 for western blot (cat. sc-30002), and horseradish peroxidase-labeled goat anti-rabbit antibodies (cat sc-2004) were obtained from Santa Cruz Biotechnology Inc. (Santa Cruz, CA). Antibodies against the TLR-4 receptor (cat. Sc-13591) blocking its activity were supplied by Santa Cruz Biotechnology Inc. Antibodies against the CD44 receptor (cat. MABT78) blocking its activity were supplied by Millipore Corporation (Billerica, MA).

Uric acid (UA) (U0881), and SOD (S5395) were obtained from Sigma-Aldrich S.r.l. (Milan, Italy). Mouse IL-1β (cat. IB49700), and IL-6 (cat. 27768) commercial ELISA kits were provided by Immuno-Biological laboratories Inc. (Minneapolis, MN). Mouse MMP-13 (cat. E0099 m) and iNOS (cat. E0837Mu) commercial ELISA kits were obtained from USCN Life Science Inc. Wuhan (Wuhan, China). HA ELISA kit (cat n° K-1200) was obtained by Echelon Biosciences Inc. (Salt Like City, UT). High molecular weight HA (3,000 kDa) was purchased from Sigma-Aldrich S.r.l, and, using a previous published method, for the preparation of HA at different molecular weight [Gao et al., 2006]. All other reagents used were purchased from Fluka (division of Sigma-Aldrich).

INDUCTION OF CIA AND ARTHRITIS EVALUATION

Mice were injected intradermally at the tail base with 100 μl of 2.0 mg/ml type II collagen emulsion in Freund's complete adjuvant containing 2.5 mg/ml heat-killed Mycobacterium tuberculosis H37Ra. Mice were immunized a second time 7 days later.

The severity of the arthritis in each limb was graded daily on a scale of 0–4 as follows: 0, no macroscopic signs of arthritis; 1, swelling of one group of joints (i.e., Knee or ankle joints); 2, two groups of swollen joints; 3, three groups of swollen joints; 4 swelling of the entire limb. The maximum score for each mouse was 16. Clinical severity was also assessed by quantifying changes in limb volume. Measurements were performed using a dial gauge caliper. At the end of the experimental period (day 35), the mice with maximum score (16) were chosen, anesthetized with ethyl ether and then sacrificed to remove their hind limbs.

ISOLATION AND CULTURE OF SYNOVIAL FIBROBLASTS

Synovial fibroblasts were isolated and cultured as previously described [Wooley et al., 1989]. Briefly, on day 35, the synovium of the knee joint from control mice and CIA mice was dissected and then digested with 1.0 mg/ml collagenase in DMEM with 1% FCS medium at 37°C for 2 h. The tissues were pooled, digested, and then suspended and passed through nylon mesh, in order to remove tissue debris. Dissociated cells were then washed with DMEM medium containing 50.0 μM 2-mercaptoethanol, 5.0 mM sodium pyruvate, and 10% heat inactivated FCS. Fibroblasts were then cultured overnight and non-adherent cells were then discarded. At confluence, fibroblasts were trypsinized, subdivided, and re-plated.

Synovial fibroblasts were plated at a density of 10^5 cells/well in a 96-well plate in DMEM medium with 1% FCS and cultured with or without the addition of TNF-α. Synovial fibroblasts were used between the third and the fifth passage in these experiments, when they constituted a homogenous population of cells.

CELL TREATMENT

Twelve hours after plating (time 0) TNF-α (5.0 ng/ml) was added, both in NSF and RASF. In cells receiving HYAL1, HYAL2, and HYAL3 siRNA (siRNAs), the treatment was performed 48 h before TNF-α, in order to block the mRNA activity of HYALs. Antioxidant (ANTIOX) treatment was performed using a mixing solution containing UA (30.0 μg/ml) and SOD (25.0 U/ml). ANTIOX solution

was added to cultures 15 min after TNF-α treatment. Finally, the cells and medium underwent biochemical evaluation 24 h after the last treatment. The study therefore included the following groups of cells: A first set of five NSF groups (NSF; NSF + TNF-α; NSF + TNF-α + ANTIOX; NSF + siRNAs + TNF-α; NSF + siRNAs + TNF-α + ANTIOX) and a second set of five RASF groups (RASF; RASF + TNF-α; RASF + TNF-α + ANTIOX; RASF + siRNAs + TNF-α; RASF + siRNAs + TNF-α + ANTIOX). A further group of cells were also used to evaluate the effect of TNF-α stimulation, siRNAs and/or antioxidant treatment on NSF and RASF after the block of TLR-4 and CD44 receptor with specific antibodies. Antibodies against TLR4 and CD44 were administered at dose of 25 μg/ml (total anti-TLR4 plus anti-CD44 50 μg/ml).

MALONDIALDEHYDE DETERMINATION

Measurement of malondialdehyde (MDA) in the cell lysate samples was performed to estimate the extension of lipid peroxidation due to free radical production in the NSF and RASF cultures. $4–5 \times 10^6$ cell samples obtained at the end of the experiments were collected in 500 μl of PBS containing 200 μM butylated hydroxytoluene and were frozen at −80°C until the assay. The day of analysis, after thawing, cell samples were centrifuged at 500*g* for 5 min at 4°C. The pellet was re-suspended and sonicated in 250 μl of sterile H_2O (Transsonic Model 420, Elma instrumentation, Germany). Lipid peroxidation evaluation was carried out according to the manufacturer's protocol of a colorimetric commercial kit (Bioxytech MDA 586 assay kit, cat.n°21044, Oxis Research Inc. Foster City, CA). The concentration of MDA in cell samples was expressed as nmol/mg protein.

siRNA TREATMENT

For siRNA experiments, 4×10^6 cells were transfected with HYAL1 siRNA, HYAL2 siRNA, and HYAL3 siRNA following the siRNA Transfection Protocol (Santa Cruz Biotechnology Inc.) with some modifications. Scramble siRNA was used under the same conditions as a negative control. After transfection, cells were seeded in six-well plates in 10% FCS/DMEM and allowed to adhere for 12 h. Culture medium was then replaced with fresh 10% FCS/DMEM for a further 12-h period. Cells were serum starved for 24 h before TNF-α was added.

RNA ISOLATION, cDNA SYNTHESIS, AND REAL-TIME QUANTITATIVE PCR AMPLIFICATION

Total RNA was isolated from NSF and RASF for reverse-PCR real time analysis of TLR-4, CD44, IL-1β, IL-6, MMP-13, iNOS, HYAL1, HYAL2, and HYAL3 (RealTime PCR system, Mod. 7500, Applied Biosystems, Foster City, CA) using an Omnizol Reagent Kit (Euroclone, Vetherby, West York, UK). The first strand of cDNA was synthesized from 1.0 μg total RNA using a high capacity cDNA Archive kit (Applied Biosystems). β-actin mRNA was used as an endogenous control to allow the relative quantification of TLR-4, CD44, IL-1β, IL-6, MMP-13, iNOS, HYAL1, HYAL2, and HYAL3. PCR RealTime was performed by means of ready-to-use assays (Assays on demand, Applied Biosystems) on both targets and endogenous controls. The amplified PCR products were quantified by measuring the calculated cycle thresholds (C_T) of TLR-4, CD44, IL-1β, IL-6, MMP-13, iNOS, HYAL1, HYAL2, HYAL3, and β-Actin mRNA. The C_T values were plotted against the log input RNA concentration in serially diluted total RNA of synovial fibroblast samples and used to generate standard curves for all mRNAs analyzed. The amounts of specific mRNA in samples were calculated from the standard curve and normalized with β-actin mRNA. After normalization, the mean value of NSF levels became the calibrator (one per sample) and the results are expressed as the n-fold difference relative to normal controls (relative expression levels).

WESTERN BLOT ASSAY OF TLR-4 AND CD44 PROTEINS

For SDS–PAGE and Western blotting, NSF and RASF were washed twice in ice-cold PBS and subsequently dissolved in SDS sample buffer (62.5 mM Tris/HCl, pH 6.8, 2% w/v SDS, 10% glycerol, 50 mM dithiothreitol, 0.01% w/v bromophenol blue). β-actin protein was used as an endogenous control to allow the normalization of TLR-4 and CD44 proteins. Aliquots of the protein extracted (10–25 μl/well) were separated on a mini gel (10%). The proteins were blotted onto polyvinylidene difluoride membranes (GE Healthcare Europe GmbH, Munich, Germany) using a semi-dry apparatus (Bio-Rad, Hercules, CA). The blots were transferred to a blocking buffer solution (1× PBS, 0.1% Tween 20, 5% w/v non-fat dried milk) and incubated for 1 h. The membranes were then incubated with specific diluted (1:1) primary antibody in 5% bovine serum albumin, 1× PBS, and 0.1% Tween 20 and stored in a roller bottle at 4°C overnight. After the blots were washed in three stages in wash buffer (1× PBS, 0.1% Tween 20), they were incubated with the diluted (1:5,000) secondary polyclonal antibody in TBS/Tween-20 buffer containing 5% non-fat dried milk. After 45 min of gentle shaking, the blots were washed five times in wash buffer and the proteins were made visible using a UV/visible transilluminator (EuroClone) and Kodak BioMax MR films. A densitometric analysis was also run in order to quantify each band.

NF-kB p50/65 TRANSCRIPTION FACTOR ASSAY

NF-kB p50/65 DNA binding activity in nuclear extracts of NSF and RASF was evaluated in order to measure the degree of NF-kB activation. The analysis was carried out following the manufacturer's protocol for a commercial kit (NF-kB p50/65 EZ-TFA Transcription Factor Assay Colorimetric, cat. n°70-510, Millipore, Billerica, MA). In brief, cytosolic and nuclear extraction was performed by lysing the cell membrane with an apposite hypotonic lysis buffer containing protease inhibitor cocktail and tributylphosphine (TBP) as reducing agent. After centrifugation at 8,000*g*, the supernatant containing the cytosolic fraction was stored at −80°C, while the pellet containing the nuclear portion was then re-suspended in the apposite extraction buffer and the nuclei were disrupted by a series of drawing and ejecting actions. After incubation with primary and secondary antibodies, color development was observed following the addition of the substrate TMB/E. Lastly, the absorbance of the samples was measured using a spectrophotometric microplate reader set at λ 450 nm. Values are expressed as relative optical density (OD) per mg protein.

IL-1-β, IL-6, MMP-13, AND INOS ELISA ASSAY

The analysis of IL-1β and IL-6 was carried out using a specific commercial kit. For IL-1β 50 μl of standards, samples and controls were added to each well of the coated microplate. Fifty microliter of each specific biotin-conjugate antibody was then added to each well. After 120 min incubation at 20–22°C, the liquid from the wells was discarded, the wells were washed three times and 100 μl of Streptavidin-HRP was added. After further incubation for 60 min and washing the wells again, 100 μl of a substrate chromogen solution was added. After 10 min incubation and the addition of 100 μl of stop solution, the absorbance of each well was read spectrophotometrically at λ 450 nm. IL-1β values are expressed as pg/ml. For the assay of IL-6, 100 μl of standards, samples and controls were added to each well of the coated microplate. Then 100 μl of the biotin-conjugate antibody was added to each well. After overnight incubation at 4°C, the liquid from the wells was discarded, the wells were washed and 100 μl of Streptavidin-HRP was then added. After further incubation for 30 min at 4°C and washing the wells again, 100 μl of a substrate chromogen solution was added to each well. After 30 min incubation at room temperature and the addition of 100 μl of stop solution, the absorbance of each well was read spectrophotometrically at λ 450 nm within 30 min. IL-6 values are expressed as pg/ml. MMP-13 and iNOS evaluation was performed by following manufacturer's instructions. MMP-13 values are expressed as pg/mg protein, while iNOS values are expressed as U/mg protein.

HA ASSAY

HA analysis assay was carried out using a specific enzyme-linked binding protein assay test kit. In brief, 100 μl of samples and standards to an uncoated 96-well polystyrene plate, including diluent buffer as blank controls were added. Then 50 μl of detector buffer to all samples and standards except the blank are also added. After mixing gently, the plate was covered with plate seal and incubated for 30 min at 37°C. Following the incubation, 100 μl of controls and samples to the corresponding well of the Detection Plate were added. After mixing contents, the plate was covered with seal and incubated for 30 min at 37°C. Then after discarding the liquid from the wells, and washing four times with the wash buffer solution, 100 μl of working enzyme to each well were added. The contents were mixed, covered and incubated for 30 min at 37°C. Then, after washing the Detection Plate four times with the wash buffer, 100 μl of working substrate to each well were added. After a brief incubation in the dark at room temperature, the reaction was stopped by adding 50 μl of stop solution to each well. Absorbance was read, within 15 min, at 405 nm using a microplate reader (DAS srl, Rome, Italy). The concentration of HA in each sample was determined by interpolation from a standard curve ranging from 25.0 to 200.0 ng/ml.

HA SIZE ANALYSIS

Purification of HA from culture medium sample was carried out as previously described [Lee and Cowman, 1994]. Briefly, 5.0 ml of each sample were first subjected to Pronase treatment (GIBCO, Carlsband, CA), at concentration of 38 mg/ml in 0.15 M NaCl. In a (v/c) ratio, followed by incubation at 37°C for 5 h and filtration through a 0.45 mm nylon membrane. The HA size was evaluated by agarose and polyacrylamide gel electrophoresis (1.5–4.0%, 1×TBE buffer, pH = 7.9, 40 to 400 V) using previously published methods [Bhilocha et al., 2011; Cowman et al., 2011], with some modifications. In brief, purified samples containing HA were dried in a vacuum drier (CentriVap Console, Labconco Corporation, Kansas City, MO) and the pellet was re-suspended with 10 μl of buffered solution and then loaded per lane. Defined HA ladder at different molecular weight (1, 2, 5, 50, 150, 500, 2,000 and 3,000 kDa) were also run as standards. After electrophoresis, the gel was removed from the apparatus, stained with Stains-All dye (0.005% w/v in ethanol), and then illuminated in a dark room connected up to a digital camera (mod. Coolpix 4500, Tokyo, Japan). Data were acquired and processed by the computer using a specific data acquisition program (Nikon view 5).

PROTEIN DETERMINATION

The amount of protein was determined using the Bio-Rad protein assay system (Bio-Rad Lab. Inc., Richmond, CA) with bovine serum albumin as a standard, in accordance with the published method [Bradford, 1976].

STATISTICAL ANALYSIS

Data are expressed as the mean ± S.D. values of at least seven experiments for each test. All assays were repeated three times to ensure reproducibility. Statistical analysis was performed by one-way analysis of variance (ANOVA) followed by the Student–Newman–Keuls test. The statistical significance of differences was set at $P < 0.05$.

STATEMENT OF ANIMAL CARE

The studies reported in this article were carried out in accordance with the Helsinki declaration and the NIH guidelines for the Care and Use of Laboratory Animals.

RESULTS

TLR-4 AND CD44 mRNA EXPRESSION AND WESTERN BLOT ANALYSIS

TLR-4 and CD44 mRNA evaluation (Figs. 1 and 2, panel A of each Figure) and Western blot analysis with densitometric evaluation (Figs. 1 and 2, panels B and C of each Figure) were assayed in order to estimate the degree of TLR-4 and CD44 activation in NSF and RASF after stimulation with TNF-α. The results showed a significant increase in the expression and protein synthesis of both TLR-4 and CD44 receptor in NSF treated with TNF-α (Figs. 1 and 2). The addition of the antioxidant mixture significantly reduced the expression of TLR-4 and of CD44, in both NSF and RASF stimulated with TNF-α. These data indicate that the reduction of the detrimental peroxynitrites and superoxide anions, which are in part responsible for HA degradation, may significantly reduce TLR-4 and CD44 activation. In NSF, the pre-treatment with siRNAs 48 h before TNF-α significantly reduced TLR-4 and CD44 expression, but did not fully abolish the expression of the two receptors exerted by TNF-α action. The same trend was also observed for RASF treated with siRNAs plus TNF-α. In fact, compared to NSF, RASF showed a similar behavior in

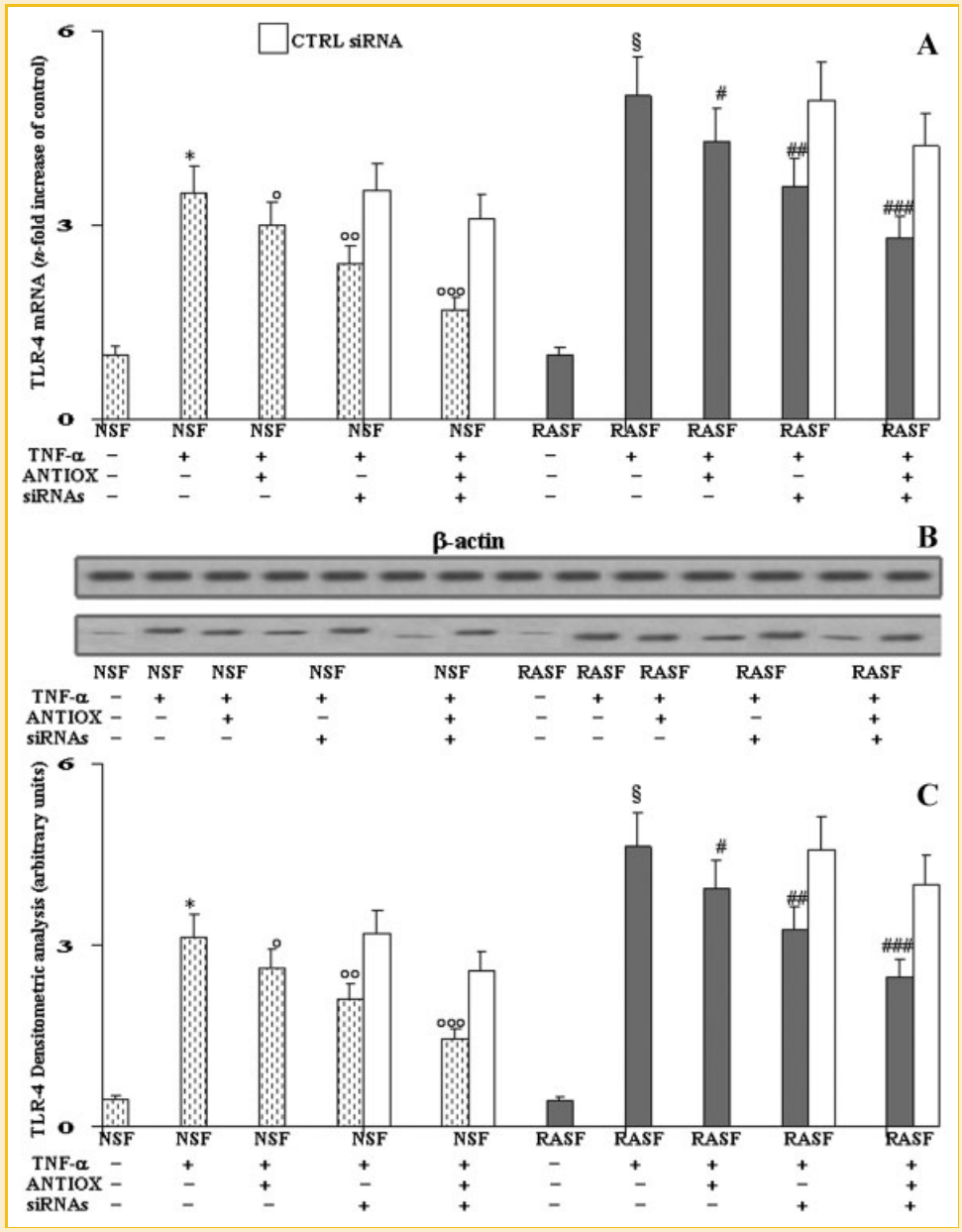

Fig. 1. Effect of TNF-α stimulation, siRNAs, and/or antioxidant treatment on NSF and RASF TLR-4 mRNA expression (A) and related protein production (B, C). Values are the mean ± S.D. of no less than seven experiments and are expressed as the n-fold increase with respect to the Control (A) and as both Densitometric analysis (C) and Western Blot analysis (B) for the TLR-4 protein levels. White bars represent control siRNA. $^{*}P < 0.001$ versus Control (NSF); $^{\circ}P < 0.001$ versus NSF + TNF-α; $^{\circ\circ}P < 0.001$ versus NSF + TNF-α and versus NSF + TNF-α + ANTIOX; $^{\circ\circ\circ}P < 0.001$ versus NSF + TNF-α + siRNAs and versus NSF + TNF-α + ANTIOX; $^{\S}P < 0.001$ versus RASF; $^{\#}P < 0.001$ versus RASF + TNF-α; $^{\#\#}P < 0.001$ versus RASF + TNF-α and versus RASF + TNF-α + ANTIOX; $^{\#\#\#}P < 0.001$ versus RASF + TNF-α + siRNAs and versus RASF + TNF-α + ANTIOX.

CD44 and TLR-4 mRNA expression and the related proteins after siRNA treatment. However, the increase in TLR-4 and CD44 expression and protein production was greater in RASF with respect to NSF. Finally, the treatment of cells with the antioxidant mixture, pre-treated with HYAL siRNAs and stimulated with TNF-α showed the lowest degree of TLR-4 and CD44 expression with respect to antioxidant or siRNA treatment alone, indicating that the blocking of both pathways of HA degradation may lead to a large reduction in the small HA fragments that stimulate TLR-4 and CD44 receptors. Although basal levels of TLR-4 and CD44 expression in the RASF were not greater than those for NSF, TNF-α stimulation produced an over expression of these two receptors which was higher in NSF than in RASF, suggesting an up-regulation due to CIA.

LIPID PEROXIDATION ANALYSIS

Determination of MDA was performed to estimate the degree of free radical production on NSF and RASF culture at end of the experiments (Fig. 3). Low levels of MDA were found in the control wells and these values were considered physiological. In contrast, a significant increase in MDA production was seen in both NSF and

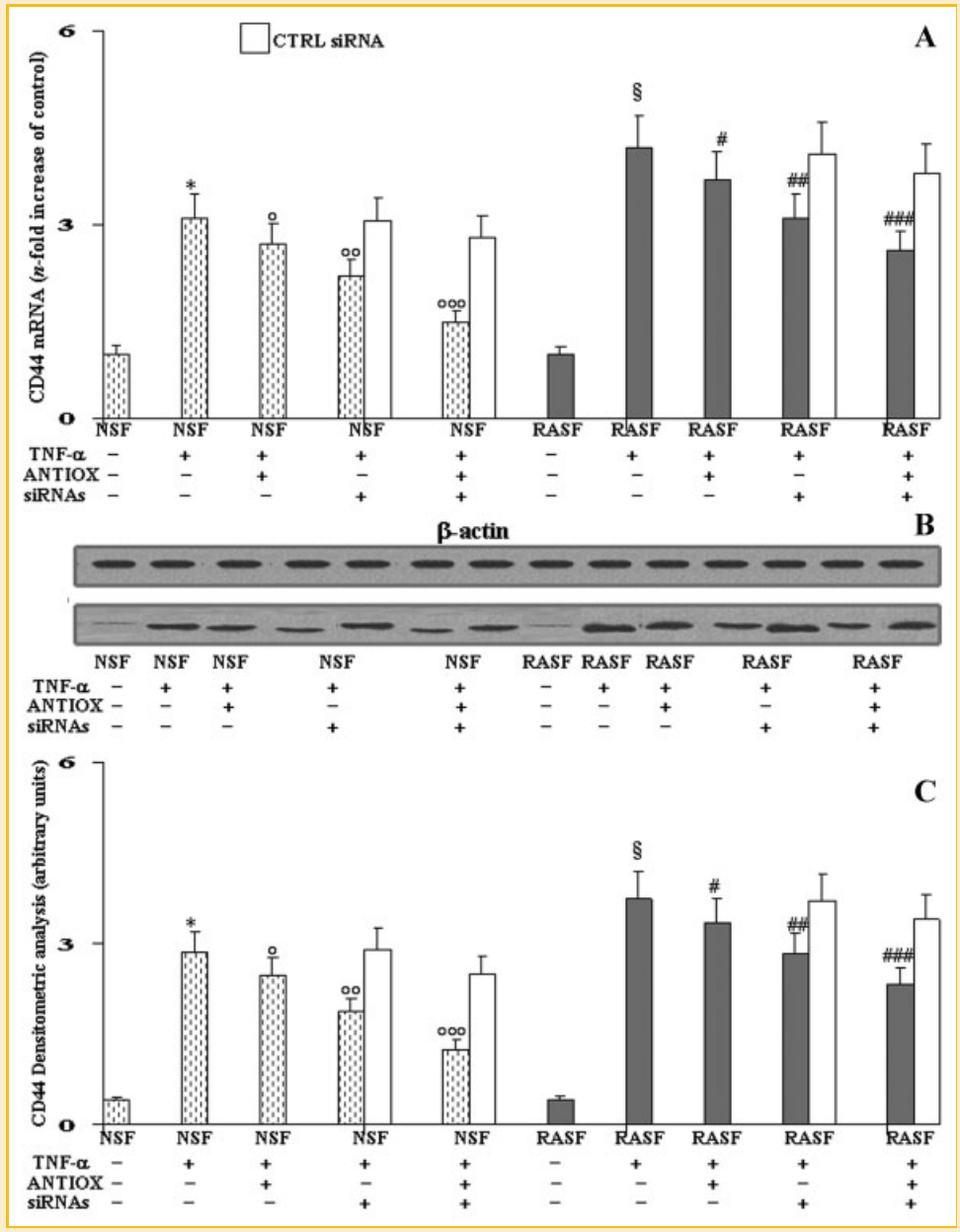

Fig. 2. Effect of TNF-α stimulation, siRNAs, and/or antioxidant treatment on NSF and RASF CD44 mRNA expression (A) and related protein production (B, C). Values are the mean ± S.D. of no less than seven experiments and are expressed as the n-fold increase with respect to the Control (A) and as both Densitometric analysis (C) and Western Blot analysis (B) for the CD44 protein levels. White bars represent control siRNA. $^{*}P < 0.001$ versus Control (NSF); $^{\circ}P < 0.001$ versus NSF + TNF-α; $^{\circ\circ}P < 0.001$ versus NSF + TNF-α and versus NSF + TNF-α + ANTIOX; $^{\circ\circ\circ}P < 0.001$ versus NSF + TNF-α + siRNAs and versus NSF + TNF-α + ANTIOX; $^{\S}P < 0.001$ versus RASF; $^{\#}P < 0.001$ versus RASF + TNF-α; $^{\#\#}P < 0.001$ versus RASF + TNF-α and versus RASF + TNF-α + ANTIOX; $^{\#\#\#}P < 0.001$ versus RASF + TNF-α + siRNAs and versus RASF + TNF-α + ANTIOX.

RASF stimulated with TNF-α, although the MDA levels were higher in RASF than NSF. The antioxidant treatment was able to reduce free radical action, induced by TNF-α treatment, in all group of cells, while siRNAs pre-treatment did not exert any influence on MDA levels.

NF-KB ACTIVATION

Figure 4 shows the changes in the NF-kB p50/p65 heterodimer translocation in NSF and RASF over the course of the experiment. This assay was performed mainly in order to evaluate the initiation of the inflammatory process, since the NF-kB factor can be activated by both the TLR-4 and CD44 pathways, which in turn may converge to transcribe the expression of several genes that prime/amplify the inflammatory response. The data obtained by assaying the NF-kB factor confirmed that TNF-α stimulation was able to activate NF-kB expression via both TLR-4 and CD44 receptors, since their expression was significantly high. NF-kB activation was greater in RASF than in NSF, the obvious consequence of a higher activation of TLR-4 and CD44 in RASF than in NSF (Figs. 1 and 2). The pre-treatment of both NSF and RASF with siRNAs significantly reduced the TNF-α effect, and the addition of the antioxidant mixture further

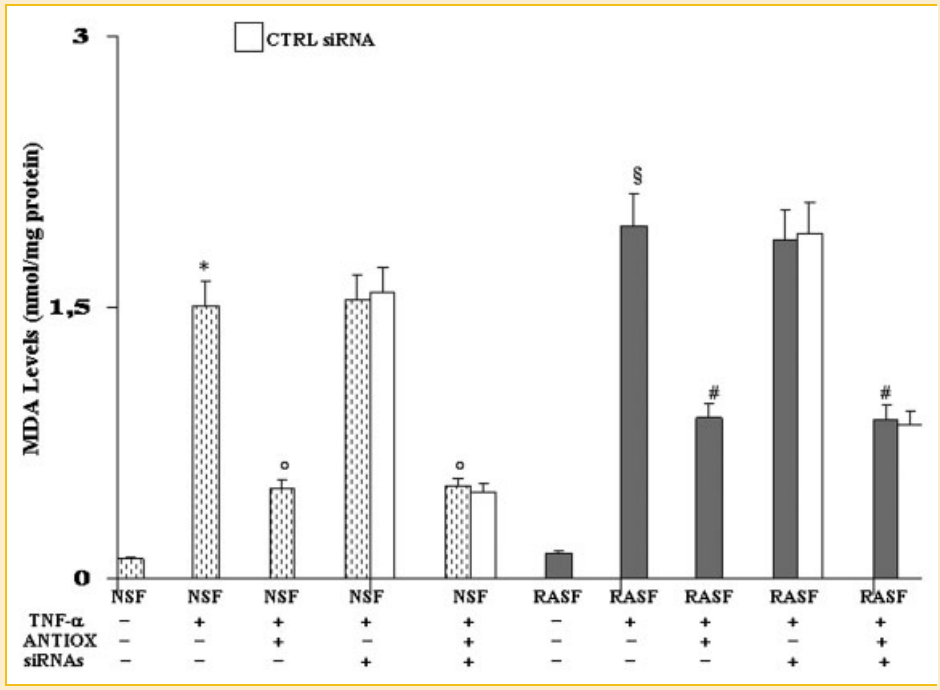

Fig. 3. Effect of TNF-α stimulation, siRNAs, and/or antioxidant treatment on NSF and RASF MDA levels. Values are the mean ± S.D. of no less than seven experiments and are expressed as nmol/mg protein. White bars represent control siRNA $^{*}P < 0.001$ versus Control (NSF); $^{\circ}P < 0.001$ versus NSF + TNF-α; $^{\S}P < 0.001$ versus RASF; $^{\#}P < 0.001$ versus RASF + TNF-α.

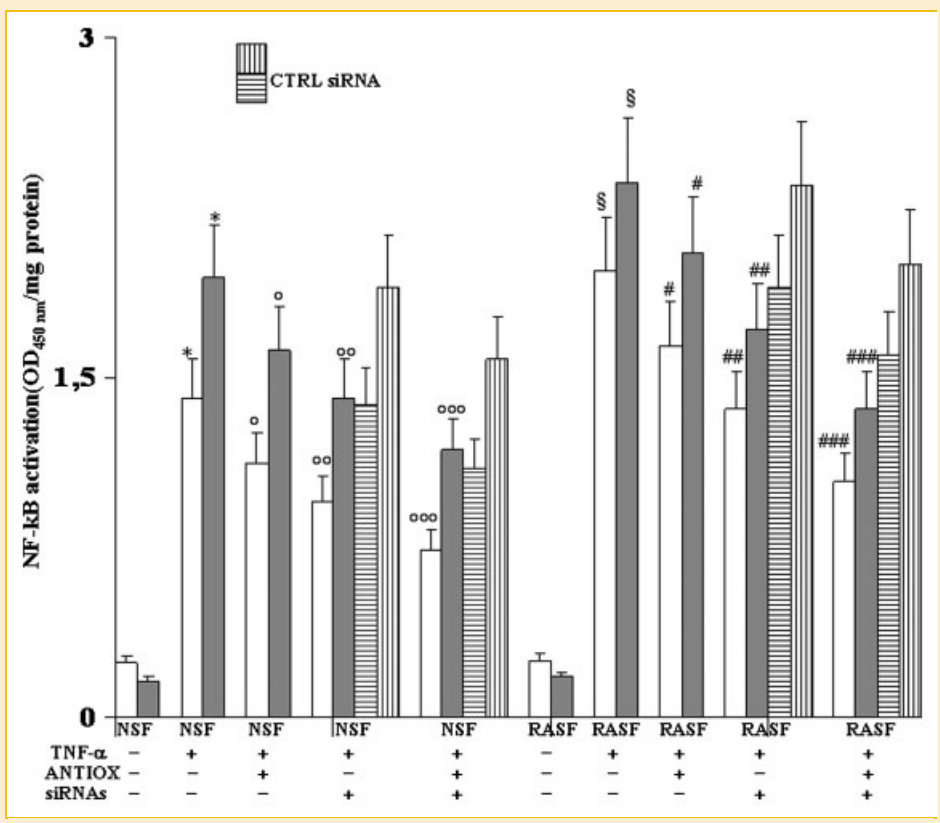

Fig. 4. Effect of TNF-α stimulation, siRNAs, and/or antioxidant treatment on NSF and RASF NF-kB p50/65 transcription factor DNA binding activity. White bars represent the p/50 subunit, gray bars represent the p/65 subunit. Bars with horizontal lines and bars with vertical lines represent control siRNA, p/50 and p/65, respectively. Values are the mean ± S.D. of no less than seven experiments and are expressed as Optical Density at λ 450 nm/mg protein of nuclear extract. $^{*}P < 0.001$ versus Control (NSF); $^{\circ}P < 0.001$ versus NSF + TNF-α; $^{\circ\circ}P < 0.001$ versus NSF + TNF-α and versus NSF + TNF-α + ANTIOX; $^{\circ\circ\circ}P < 0.001$ versus NSF + TNF-α + siRNAs and versus NSF + TNF-α + ANTIOX; $^{\S}P < 0.001$ versus RASF; $^{\#}P < 0.001$ versus RASF + TNF-α; $^{\#\#}P < 0.001$ versus RASF + TNF-α and versus RASF + TNF-α + ANTIOX; $^{\#\#\#}P < 0.001$ versus RASF + TNF-α + siRNAs and versus RASF + TNF-α + ANTIOX.

decreased NF-kB activation as a result of a lower production of HA fragments. The reduction of NF-kB in TNF-α stimulated cells by HYAL siRNAs and/or the antioxidant mixture confirms the involvement of NF-kB in the mediation of the inflammatory process activated by TLR-4 and CD44-, as well as the initial mediation through degraded HA.

INFLAMMATORY CYTOKINES, MMP-13, AND iNOS mRNA EXPRESSION AND PROTEIN LEVELS

IL-1β (Fig. 5), IL-6 (Fig. 6), MMP-13 (Fig. 7), and iNOS (Fig. 8) mRNA evaluation (panel A of each Figure), and ELISA assay (panel B of each Figure) confirmed the previous data obtained from evaluating the NF-kB factor, TLR-4, and CD44. As the Figures show, a significant increase in the expression and protein synthesis of inflammatory cytokines, MMP-13 and iNOS was found in NSF treated with TNF-α. This increment may be considered to be the direct consequence of TLR-4 and CD44 activation by degraded native HA, exerted by HYALs and ROS, that in turn stimulate NF-kB translocation into the nucleus. NF-kB translocation may then stimulate IL-1β, IL-6, MMP-13, and iNOS gene expression. Pre-treatment of NSF with the HYAL siRNAs, and/or the antioxidant mixture, significantly reduced levels of inflammatory cytokines, MMP-13 and iNOS as a probable consequence of the reduction in interaction between small HA fragments with TLR-4 and

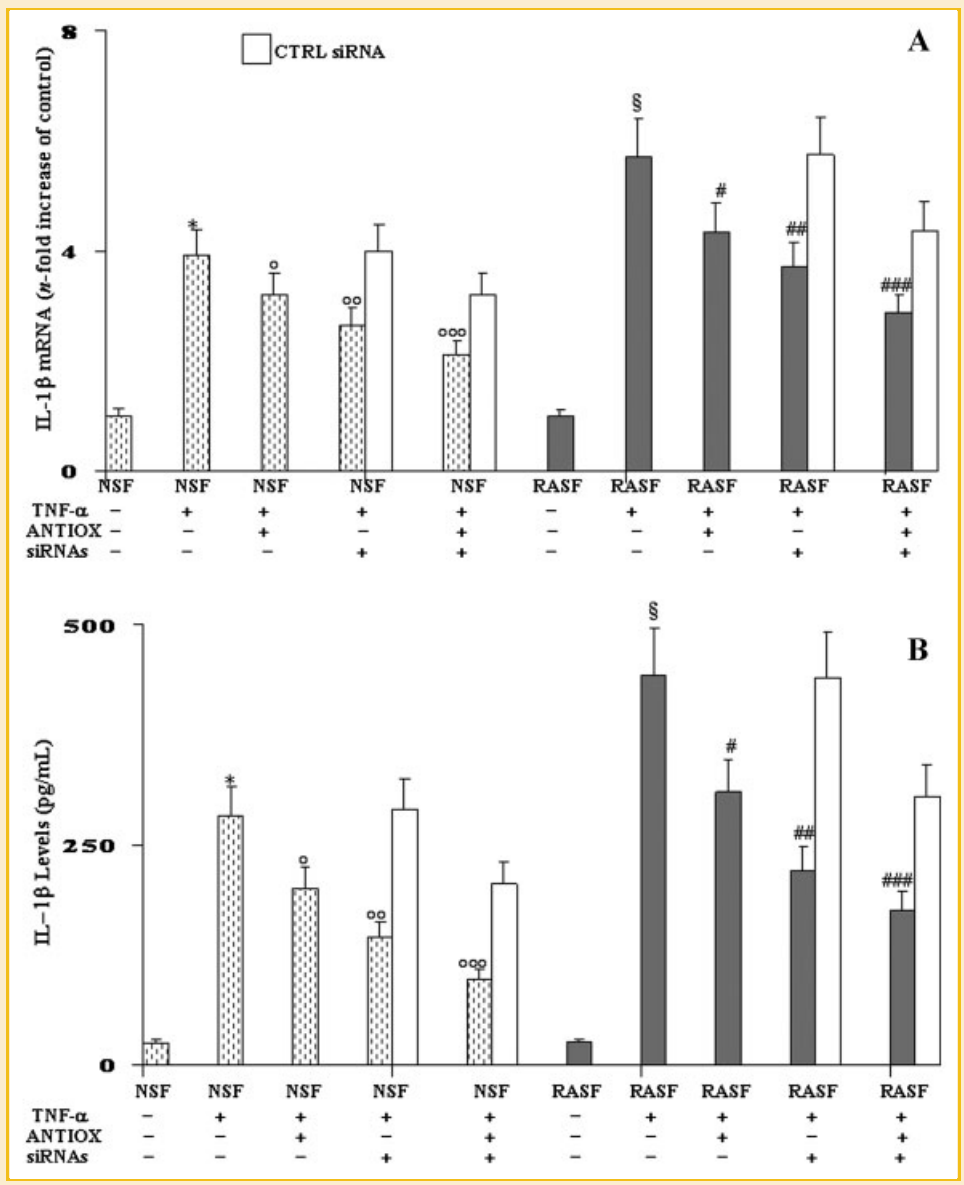

Fig. 5. Effect of TNF-α stimulation, siRNAs, and/or antioxidant treatment on NSF and RASF IL-1β mRNA expression (A) and related protein production (B). Values are the mean ± S.D. of no less than seven experiments and are expressed as the n-fold increase with respect to the Control (A) and as pg/ml (B) for the IL-1β protein levels. White bars represent control siRNA. $^{*}P < 0.001$ versus Control (NSF); $^{\circ}P < 0.001$ versus NSF + TNF-α; $^{\circ\circ}P < 0.001$ versus NSF + TNF-α and versus NSF + TNF-α + ANTIOX; $^{\circ\circ\circ}P < 0.001$ versus NSF + TNF-α + siRNAs and versus NSF + TNF-α + ANTIOX; $^{\S}P < 0.001$ versus RASF; $^{\#}P < 0.001$ versus RASF + TNF-α; $^{\#\#}P < 0.001$ versus RASF + TNF-α and versus RASF + TNF-α + ANTIOX; $^{\#\#\#}P < 0.001$ versus RASF + TNF-α + siRNAs and versus RASF + TNF-α + ANTIOX.

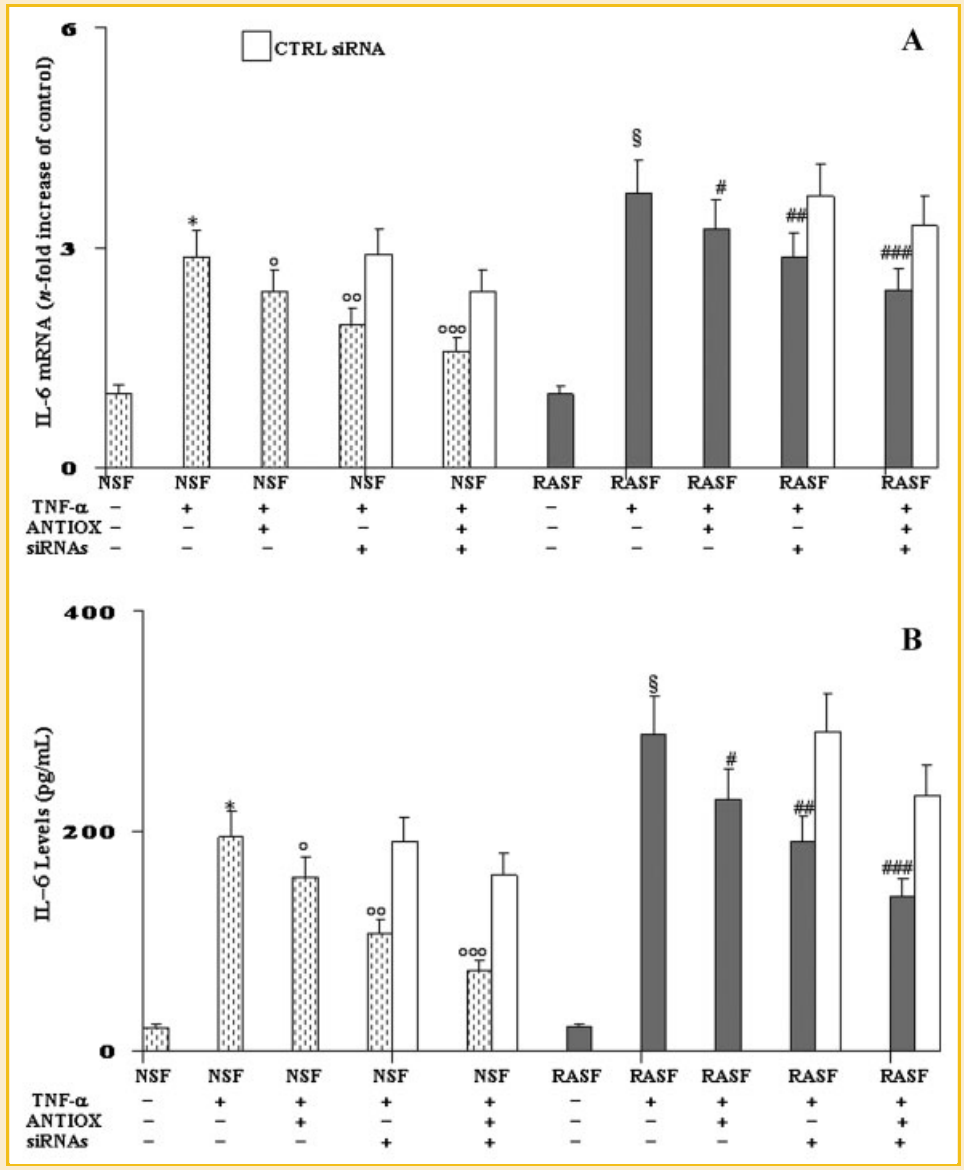

Fig. 6. Effect of TNF-α stimulation, siRNAs, and/or antioxidant treatment on NSF and RASF IL-6 mRNA expression (A) and related protein production (B). Values are the mean ± S.D. of no less than seven experiments and are expressed as the n-fold increase with respect to the Control (A) and as pg/ml (B) for the IL-6 protein levels. White bars represent control siRNA. $^{*}P < 0.001$ versus Control (NSF); $^{\circ}P < 0.001$ versus NSF + TNF-α; $^{\circ\circ}P < 0.001$ versus NSF + TNF-α and versus NSF + TNF-α + ANTIOX; $^{\circ\circ\circ}P < 0.001$ versus NSF + TNF-α + siRNAs and versus NSF + TNF-α + ANTIOX; $^{\S}P < 0.001$ versus RASF; $^{\#}P < 0.001$ versus RASF + TNF-α; $^{\#\#}P < 0.001$ versus RASF + TNF-α and versus RASF + TNF-α + ANTIOX; $^{\#\#\#}P < 0.001$ versus RASF + TNF-α + siRNAs and versus RASF + TNF-α + ANTIOX.

CD44. Comparable results were found in RASF, where IL-1β, IL-6, MMP-13, and iNOS expression was more elevated than in NSF after TNF-α treatment. The pre-treatment with HYAL siRNAs once again significantly decreased the expression of inflammatory cytokines, MMP-13, and iNOS in RASF.

HA LEVELS AND MOLECULAR WEIGHT

HA concentrations were measured in NSF and RASF medium in order to verify and confirm the inflammatory effects of degraded HA levels associated with TNF-α treatment (Fig. 9). TNF-α stimulation produced a significant increase both in NSF and RASF HA levels with respect to controls. The addition of the antioxidants and/or HYAL siRNA was able to significantly reduce HA concentrations both in NSF and RASF.

Figure 10 (panels A and B) shows the evaluation of HA molecular size in all considered groups of cells, although 1 and 2 kDa HA oligosaccharides were not revealed. Untreated cells present a comparable amount of HA at low and at high molecular weight, although high molecular weight HA was more represented. On the contrary, in cells treated with TNF-α a marked increase in the content of HA at low molecular weight and a reduction in the percentage of HA at high molecular weight was revealed, although this HA ratio inversion was more evident in RASF than in NSF. The treatment of cells with the antioxidants and/or HYALs siRNA, after

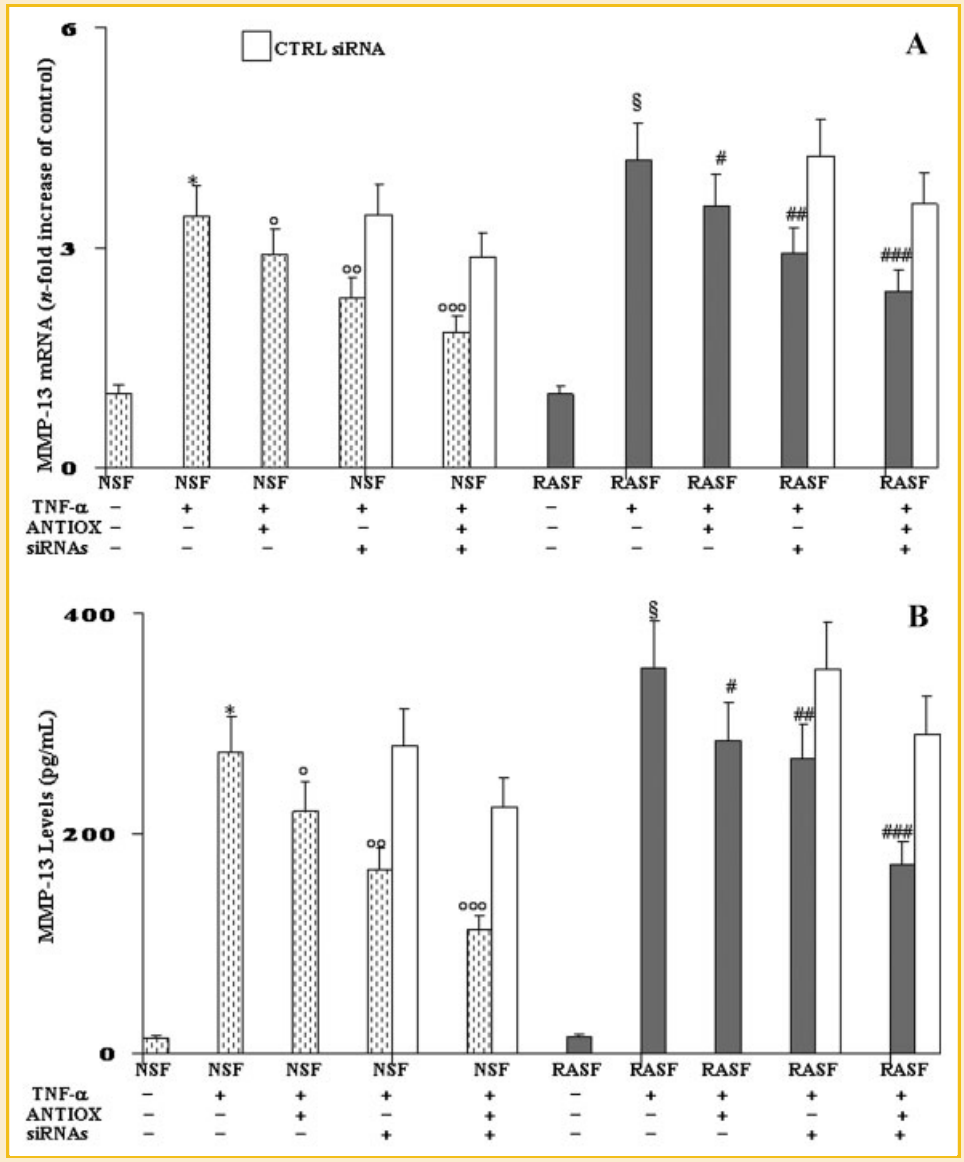

Fig. 7. Effect of TNF-α stimulation, siRNAs, and/or antioxidant treatment on NSF and RASF MMP-13 mRNA expression (A) and related protein production (B). Values are the mean ± S.D. of no less than seven experiments and are expressed as the n-fold increase with respect to the Control (A) and as pg/mlL (B) for the MMP-13 protein levels. White bars represent control siRNA. $^{*}P < 0.001$ versus Control (NSF); $^{\circ}P < 0.001$ versus NSF + TNF-α; $^{\circ\circ}P < 0.001$ versus NSF + TNF-α and versus NSF + TNF-α + ANTIOX; $^{\circ\circ\circ}P < 0.001$ versus NSF + TNF-α + siRNAs and versus NSF + TNF-α + ANTIOX; $^{\S}P < 0.001$ versus RASF; $^{\#}P < 0.001$ versus RASF + TNF-α; $^{\#\#}P < 0.001$ versus RASF + TNF-α and versus RASF + TNF-α + ANTIOX; $^{\#\#\#}P < 0.001$ versus RASF + TNF-α + siRNAs and versus RASF + TNF-α + ANTIOX.

TNF-α stimulation, was able to significantly change the high molecular weight/low molecular weight HA ratio. Therefore, the increase of HA at low molecular weight was positively correlated with the corresponding TNF-α stimulation.

HYAL1, HYAL2, AND HYAL3 mRNA EXPRESSION AND siRNA TREATMENT

Figure 11 reports HYAL1, HYAL2, and HYAL3 mRNA levels assayed in order to estimate the degree of HYAL expression in NSF and RASF after stimulation with TNF-α and HYAL siRNAs pre-treatment. The data showed a significant increase in the expression of the three enzymes with respect to controls in both NSF and RASF after TNF-α treatment. HYAL2 was expressed more highly, while HYAL1 and HYAL3 to a lesser extent (Fig. 11). However, as reported above, HYAL expression was greater in RASF than in NSF, probably due to an up-regulation of the synthesis pathway due to CIA injury. The pre-treatment of both NSF and RASF with HYAL siRNAs fully blocked HYAL activity, thereby confirming the blocking action of siRNAs during the experiments. The antioxidant treatments had no effect on HYALs in any of the groups.

EFFECT OF TLR-4 AND CD44 BLOCK ON TLR-4, CD44, AND IL-1β mRNA EXPRESSION

Figure 12 reports TLR-4, CD44, and IL-1β mRNA levels assayed after NSF and RASF treatment with specific antibodies against TLR-4 and CD44 receptors, in order to evaluate TLR-4, CD44, and IL-1β degree

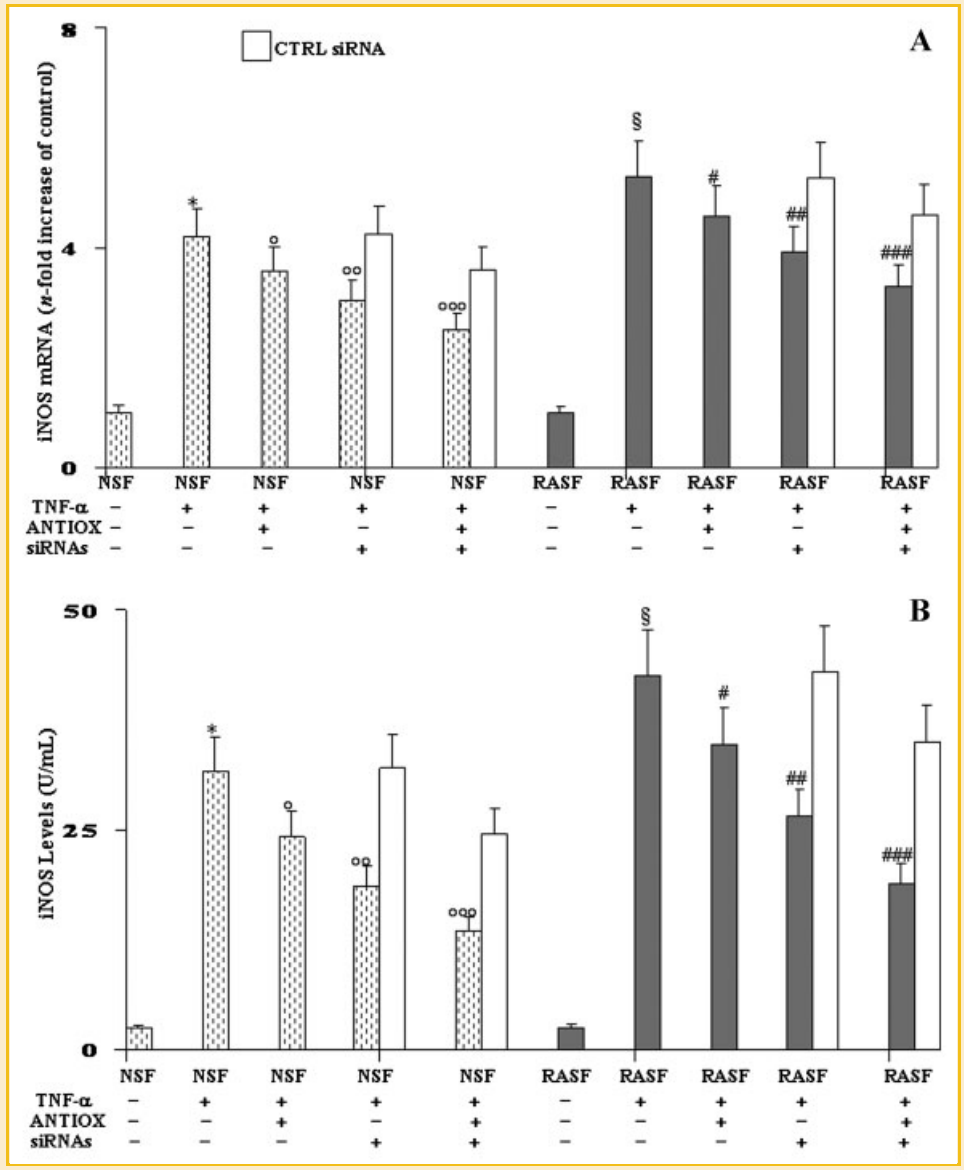

Fig. 8. Effect of TNF-α stimulation, siRNAs, and/or antioxidant treatment on NSF and RASF iNOS mRNA expression (A) and related protein production (B). Values are the mean ± S.D. of no less than seven experiments and are expressed as the n-fold increase with respect to the Control (A) and as pg/ml (B) for the iNOS protein levels. White bars represent control siRNA. $^{*}P < 0.001$ versus Control (NSF); $^{\circ}P < 0.001$ versus NSF + TNF-α; $^{\circ\circ}P < 0.001$ versus NSF + TNF-α and versus NSF + TNF-α + ANTIOX; $^{\circ\circ\circ}P < 0.001$ versus NSF + TNF-α + siRNAs and versus NSF + TNF-α + ANTIOX; $^{\S}P < 0.001$ versus RASF; $^{\#}P < 0.001$ versus RASF + TNF-α; $^{\#\#}P < 0.001$ versus RASF + TNF-α and versus RASF + TNF-α + ANTIOX; $^{\#\#\#}P < 0.001$ versus RASF + TNF-α + siRNAs and versus RASF + TNF-α + ANTIOX.

of expression in all considered groups. The data showed no expression of the two blocked receptors in all considered groups of cells. IL-1β expression, instead, was significantly increased in cells stimulated with TNF-α. The treatment with antioxidants, but not with HYALs siRNA, slightly reduced IL-1β (Fig. 12).

DISCUSSION

In the present study, we demonstrated that the products of HA degradation obtained by HYAL activity stimulated by TNF-α treatment can induce an inflammatory response in both NSF and RASF, but more intensely in RASF than in NSF. The blocking of HYAL1, HYAL2, and HYAL3 using specific siRNAs significantly reduced the inflammatory response, and the addition to cultures of an antioxidant mixture containing UA plus SOD was able to reduce inflammatory parameters. Finally, the treatment of cells with both siRNAs and the antioxidant mixture reduced the inflammatory response stimulated by TNF-α treatment to an even greater extent.

In this investigation we found a marked increase in the expression of both TLR-4 and CD44 receptors in all cells stimulated with TNF-α. The addition of the antioxidant mixture and/or the pre-treatment with specific HYAL siRNAs significantly reduced both TLR-4 and CD44 expression in each case. These data indicate that the reduction

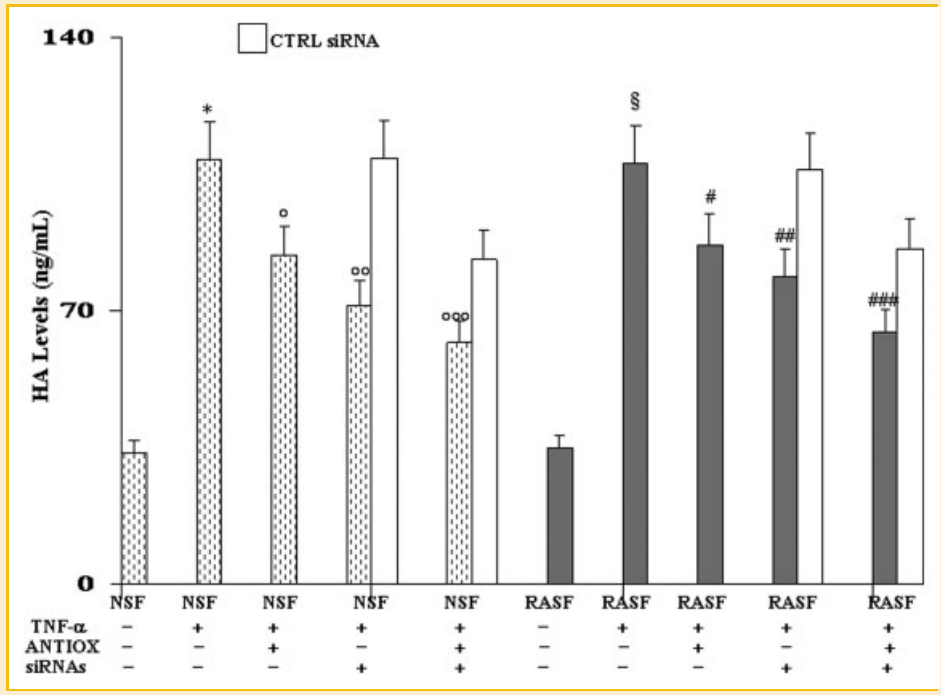

Fig. 9. Effect of TNF-α stimulation, siRNAs, and/or antioxidant treatment on NSF and RASF HA levels. Values are the mean ± S.D. of no less than seven experiments and are expressed as ng/ml. White bars represent control siRNA. $^{*}P < 0.001$ versus Control (NSF); $^{\circ}P < 0.001$ versus NSF + TNF-α; $^{\circ\circ}P < 0.001$ versus NSF + TNF-α and versus NSF + TNF-α + ANTIOX; $^{\circ\circ\circ}P < 0.001$ versus NSF + TNF-α + siRNAs and versus NSF + TNF-α + ANTIOX; $^{\S}P < 0.001$ versus RASF; $^{\#}P < 0.001$ versus RASF+ TNF-α; $^{\#\#}P < 0.001$ versus RASF + TNF-α and versus RASF + TNF-α + ANTIOX; $^{\#\#\#}P < 0.001$ versus RASF + TNF-α + siRNAs and versus RASF + TNF-α + ANTIOX.

of the detrimental peroxynitrites and superoxide anions that are in part responsible for HA degradation, and the blocking of HYALs, responsible for extended HA degradation, may significantly reduce TLR-4 and CD44 activation. These findings further support the involvement of ROS in the inflammatory mechanism, and in this case in HA degradation, as well as upholding the fundamental role played by HYALs and native HA during tissue injury.

In both NSF and RASF, the pre-treatment with siRNAs 48 h before TNF-α significantly reduced TLR-4 and CD44 expression, but did not fully abolish the expression of the two receptors exerted by TNF-α action. Compared to NSF, RASF showed a similar trend on CD44 and TLR-4 mRNA activity after the same treatment. Interestingly, in RASF, the increase in TLR-4 and CD44 expression and protein production was greater than for NSF. However, the blocking of HYALs with siRNAs was able to significantly reduce the expression of the two receptors induced by TNF-α treatment. In addition, TNF-α-stimulated cells treated with both the antioxidant mixture and pre-treated with HYAL siRNAs showed a greater reduction in TLR-4 and CD44 expression, with respect to antioxidant or siRNAs treatment alone, indicating that the blocking of both pathways for HA degradation may lead to a large reduction in the generation of small HA fragments stimulating TLR-4 and CD44 receptors.

Although no increased expression of TLR-4 and CD44 was evident in RASF, basally, an increase in the mRNA expression and the related protein synthesis of these two receptors was seen after TNF-α stimulation. This increase was higher than NSF, and could be explained as an up-regulated pathway caused by CIA injury. The addition of the siRNAs clearly blocks small HA fragment formation by preventing HA degradation. The reduction of TLR-4 and CD44 expression, stimulated by TNF-α, in both NSF and RASF, through pre-treatment with siRNAs, clearly confirms the involvement of HA fragments in the mediation of inflammatory activation of TLR-4 and CD44.

The evidence that the TLR-4 and CD44 expression was not fully abolished in both NSF and RASF, pre-treated with siRNAs and stimulated with TNF-α, could be simply explained by the hypothesis that native HA had been degraded by previously synthesized occurring HYAL. However, other pathways stimulated by TNF-α may be involved.

Results obtained from evaluating the NF-kB factor also confirmed that TNF-α stimulation was able to activate NF-kB expression via both TLR-4 and CD44 receptors. Again, NF-kB activation was higher in RASF than in NSF. This could be regarded as an obvious consequence of a higher degree of TLR-4 and CD44 stimulation by TNF-α in RASF than in NSF. Pre-treatment of both NSF and RASF with siRNAs significantly reduced the TNF-α effect, and the addition of the antioxidant mixture further decreased NF-kB activation due to the lower production of HA fragments achieved by inhibiting both degradation pathways. The decrease in NF-kB activation, in TNF-α stimulated cells, by HYAL siRNAs and/or the antioxidant mixture further supports the key role played by NF-kB on the mediation of the inflammatory response, after TLR-4 and CD44-activation, as well as providing evidence of the trigger acting through degraded HA.

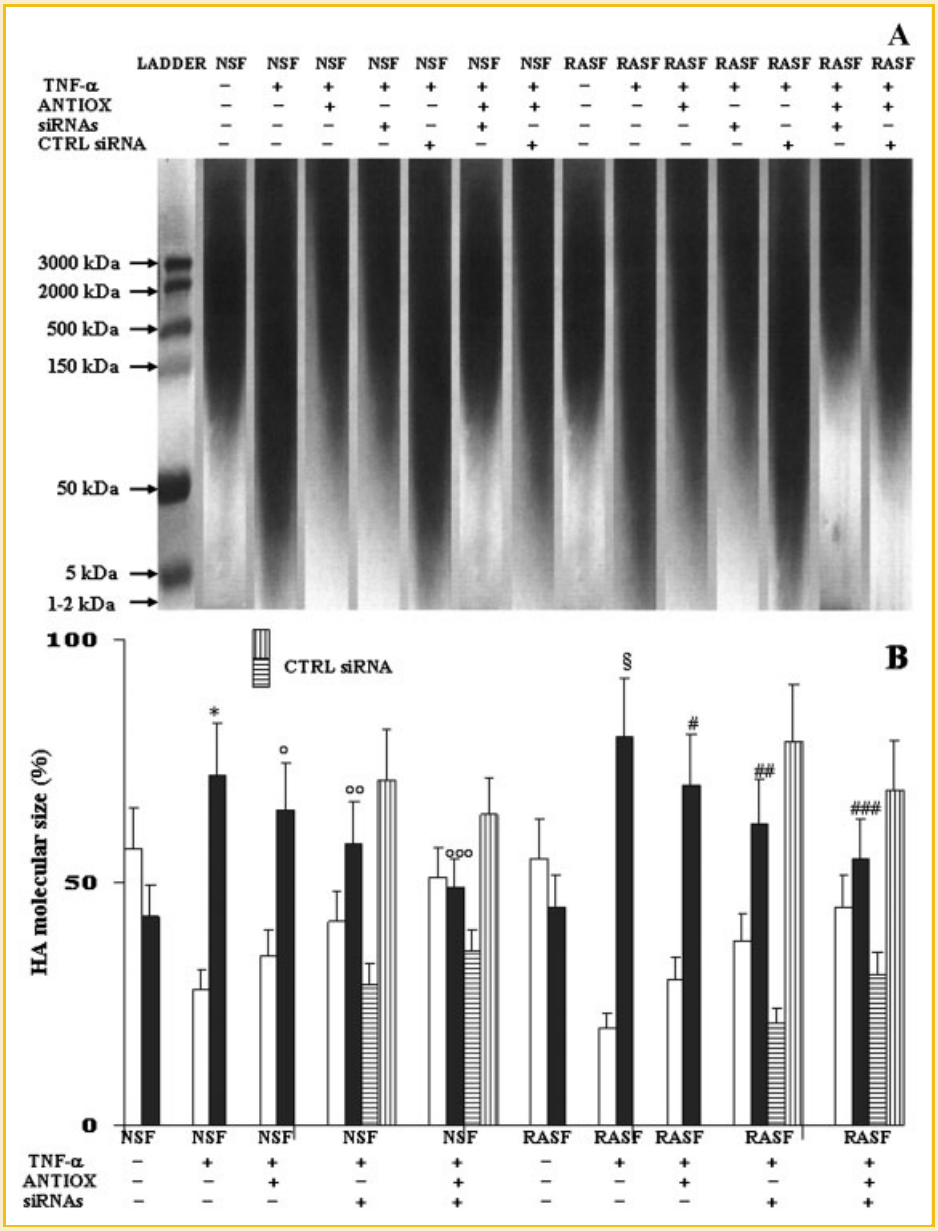

Fig. 10. Effect of TNF-α stimulation, siRNAs, and/or antioxidant treatment on NSF and RASF HA molecular size. In panel A is reported a picture of the agarose gel, while in panel B the densitometric analysis. Values are the mean ± S.D. of no less than seven experiments and are expressed as percentage (%). White bars indicate HA at high molecular weight (more than 500 kD); black bars indicate HA at low molecular weight (from 5 to 500 kD). Bars with horizontal lines and bars with vertical lines represent control siRNA, HA at high molecular weight and HA at low molecular weight, respectively. $^{*}P < 0.001$ versus Control (NSF); $^{\circ}P < 0.001$ versus NSF + TNF-α; $^{\circ\circ}P < 0.001$ versus NSF + TNF-α and versus NSF + TNF-α + ANTIOX; $^{\circ\circ\circ}P < 0.001$ versus NSF + TNF-α + siRNAs and versus NSF + TNF-α + ANTIOX; $^{\S}P < 0.001$ versus RASF; $^{\#}P < 0.001$ versus RASF+ TNF-α; $^{\#\#}P < 0.001$ versus RASF + TNF-α and versus RASF + TNF-α + ANTIOX; $^{\#\#\#}P < 0.001$ versus RASF + TNF-α + siRNAs and versus RASF + TNF-α + ANTIOX.

The evaluation of pro-inflammatory cytokines, MMP-13 and iNOS further confirmed the previous data. In fact, TNF-α stimulation induced a significant increase in the expression of these parameters. This may be due to TLR-4 and CD44 activation by small HA fragments produced by HYALs and ROS. TLR-4 and CD44 activation in turn stimulate NF-kB translocation into the nucleus. NF-kB translocation may then stimulate gene transcription resulting in increased IL-1β, IL-6, MMP-13, and iNOS. Pre-treatment of NSF with the HYAL siRNAs, and/or the antioxidant mixture, significantly reduced these inflammatory parameters, probably as a result of a reduction in the generation of small HA fragments and interaction between HA-TLR-4 and HA-CD44.

Similar data were obtained for RASF. The reduction of inflammatory parameters obtained both in NSF and RASF pre-treated with HYALs siRNAs, and/or the antioxidant mixture, and stimulated with TNF-α further demonstrate the pivotal role of HA fragments produced by HYALs and ROS degradation, in the inflammatory mechanism stimulated by TNF-α treatment.

We found a significant increase in the expression of HYALs with respect to controls after TNF-α treatment in both NSF and RASF.

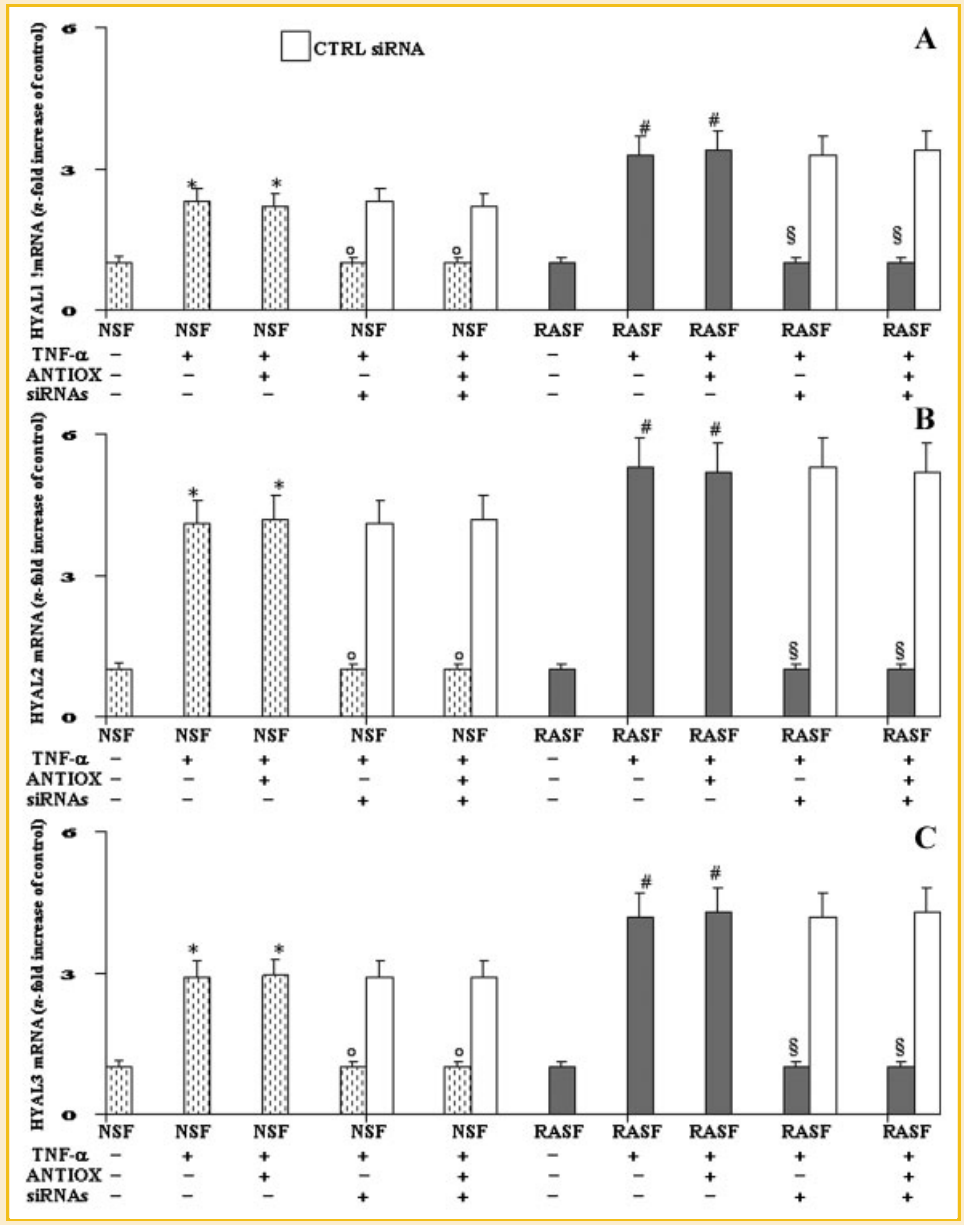

Fig. 11. Effect of TNF-α stimulation, siRNAs, and/or antioxidant treatment on NSF and RASF HYAL1 (A), HYAL2 (B), and HYAL3 (C) mRNA expression. Values are the mean ± S.D. of no less than seven experiments and are expressed as the n-fold increase with respect to the Control. White bars represent control siRNA. $^{*}P < 0.001$ versus control (NSF); $^{\circ}P < 0.001$ versus NSF + TNF-α; $^{\#}P < 0.001$ versus RASF; $^{\S}P < 0.001$ versus RASF + TNF-α.

This increase could be explained by the evidence that TNF-α increases the production of synthesizing and degrading enzymes such as HYALs and HASs, as previously reported [Campo et al., 2006; Tanimoto et al., 2010], with a probable mechanism acting in an attempt to increase biochemical activities. HYAL1 expression was less than that of HYAL2 and HYAL3. This lower HYAL1 expression could explain the minor involvement of HYAL1 in ECM degradation, or, on the contrary, that low HYAL1 expression produced a consequent low ECM degradation. However, HYAL expression was greater in RASF than in NSF, also in this case probably due to an up-regulation of the synthesis mechanism produced by CIA. Pre-treatment of both NSF and RASF with HYAL siRNAs completely blocked HYAL activity, thereby confirming the inhibitory activity of siRNAs in the experiments, while antioxidant treatment had no effect on HYALs in any of the groups.

Data about HA concentrations confirm the inflammatory effects of degraded HA levels associated with TNF-α treatment, and that the addition of the antioxidants and/or HYAL siRNA was able to significantly reduce HA concentrations both in NSF and RASF. As well as the results about the HA molecular size revealed that the cells treated with TNF-α present a significant increment in the content of HA at low molecular weight and a reduction in the percentage of HA at high molecular compared to the controls. The treatment of cells with the antioxidants and/or HYALs siRNA, after TNF-α stimulation,

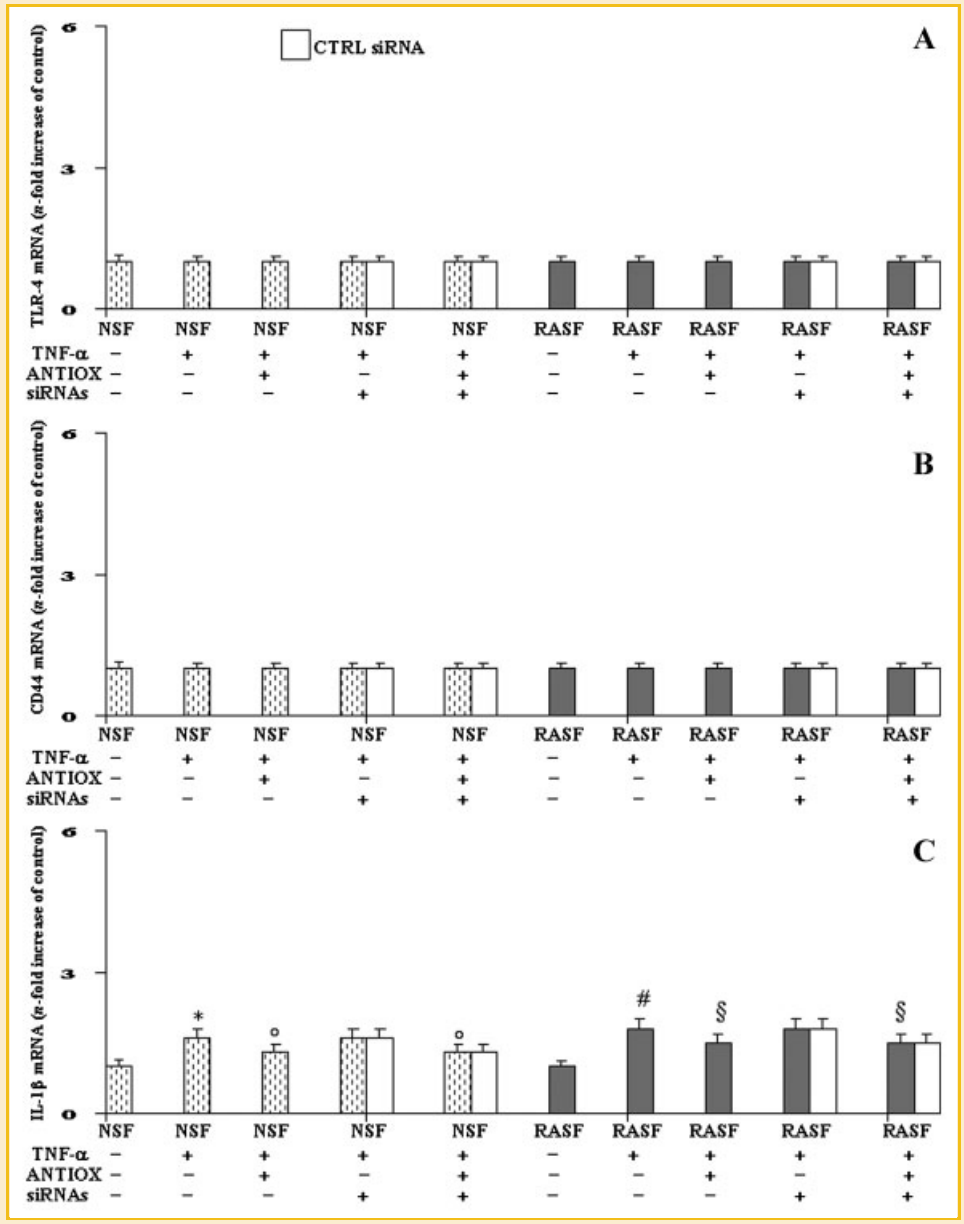

Fig. 12. Effect of TNF-α stimulation, siRNAs, and/or antioxidant treatment on NSF and RASF TLR-4 (A), CD44 (B), and IL-1β (C) mRNA expression after the block of the TLR-4 and CD44 with the specific blocking antibodies. Values are the mean ± S.D. of no less than seven experiments and are expressed as the n-fold increase with respect to the Control. White bars represent control siRNA. $^{*}P < 0.01$ versus control (NSF); $^{\circ}P < 0.05$ versus NSF + TNF-α; $^{\#}P < 0.01$ versus RASF; $^{\S}P < 0.05$ versus RASF + TNF-α.

was able to significantly limit the high molecular size/low molecular size HA ratio inversion. Hence, the increase of HA at low molecular mass was related to TNF-α stimulation. Therefore, the reduction of HA at low molecular weight exerted by antioxidants and/or HYALs siRNA can be associated with the reduction of native HA degradation.

Data about MDA levels further confirm the active role of TNF-α on free radical production, and the inhibiting activity exerted by the treatment with antioxidants. In fact, a significant increase in MDA production was found in all cells stimulated with TNF-α. The antioxidant treatment was able to significantly reduce the lipid peroxidation induced by ROS, as confirmed by the reduced MDA levels.

The treatment of NSF and RASF with specific antibodies against TLR-4 and CD44 receptors confirmed the involvement of these receptors after TNF-α stimulation. In fact, results showed no expression of the two blocked receptors in all considered groups of cells. IL-1β expression, instead, was significantly higher in cells stimulated with TNF-α. The treatment with antioxidants, but not with HYALs siRNA, slight reduced IL-1β. This result can be explained by the hypothesis that in addition to the marked effect of HA degradation to prime the inflammatory response, different other

mechanisms may stimulate cytokine transcription independently by TLR-4 and CD44 stimulation and this mechanism, involving the increase of ROS, can be limited using antioxidants. Therefore, TNF-α-induced cytokine transcription is the result of different mechanisms. However, as demonstrated by these results, HA degradation and the consequent action of the small HA fragments seem to give a strong contribution to the mediation of TNF-α-induced inflammatory response via TLR-4 and CD44.

In conclusion, the present results mean that the treatment of NSF and RASF with TNF-α activated inflammatory response through a series of different mechanisms, including HYAL and ROS stimulation that in turn degraded native high molecular weight HA. Consequently, the small HA fragments produced interacted with TLR-4 and CD44 and were thereby able to increase TLR-4 and CD44 expression and protein synthesis in both NSF and RASF. The reduction of the inflammatory parameters investigated exerted by HYALs siRNAs and/or the antioxidant mixture further support the above hypothesis.

Hence, these findings should be taken into account for future anti-inflammatory strategies although further studies are needed to fully confirm this complex mechanism.

REFERENCES

Alaniz L, Garcia M, Rizzo M, Piccioni F, Mazzolini G. 2009. Altered hyaluronan biosynthesis and cancer progression: An immunological perspective. Mini Rev Med Chem 9:1538–1546.

Bhilocha S, Amin R, Pandya M, Yuan H, Tank M, LoBello J, Shytuhina A, Wang W, Wisniewski HS, de la Motte C, Cowman MK. 2011. Agarose and polyacrilamide gel electrophoresis methods for molecular mass analysis of 5- to 500-kDa hyaluronan. Anal Biochem 417:4149.

Bradford MM. 1976. A rapid and sensitive method for the quantitation of microgram quantities of protein utilizing the principle of protein-dye binding. Anal Biochem 72:248–2254.

Campo GM, Avenoso A, Campo S, D'Ascola A, Ferlazzo AM, Calatroni A. 2006. TNF-α, IFN-γ, and IL-1β modulate hyaluronan synthase expression in human skin fibroblasts: Synergic effect by concomital treatment with $FeSO_4$ plus scorbate. Mol Cell Biochem 292:169–178.

Campo GM, Avenoso A, Campo S, D'Ascola A, Traina P, Calatroni A. 2009. Differential effect of molecular size HA in mouse chondrocytes stimulated with PMA. Biochim Biophys Acta 1790:1353–1367.

Campo GM, Avenoso A, Campo S, D'Ascola A, Nastasi G, Calatroni A. 2010a. Molecular size hyaluronan differently modulates toll-like receptor-4 in LPS-induced inflammation in mouse chondrocytes Biochimie 92:204–215.

Campo GM, Avenoso A, Campo S, D'Ascola A, Nastasi G, Calatroni A. 2010b. Small hyaluronan oligosaccharides induce inflammation by both toll-like-4 and CD44 receptors in human chondrocytes. Biochem Pharmacol 80:480–490.

Cowman MK, Chen CC, Pandya M, Yuan H, Ramkishun D, LoBello J, Bhilocha S, Russel-Puleri S, Skendaj E, Mijovic J, Jing W. 2011. Improved agarose gel electrophoresis method and molecular mass calculation for high molecular mass hyaluronan. Anal Biochem 417:50–56.

Cunnane G, FitzGerald O, Hummel KM, Youssef PP, Gay RE, Gay S, Bresnihan B. 2001. Synovial tissue protease gene expression and joint erosion in early rheumatoid arthritis. Arthritis Rheum 44:1744–1753.

Filippin LI, Vercellino R, Marroni NP, Xavier RM. 2008. Redox signalling and the inflammatory response in rheumatoid arthritis. Clin Exp Immunol 152:415–422.

Gao F, Cao M, Yang C, He Y, Liu Y. 2006. Preparation and characterization of hyaluronan oligosaccharides for angiogenesis study. J Biomed Mater Res B Appl Biomater 78:385–392.

Gaston JS. 2008. Cytokines in arthritis–the 'big numbers' move centre stage. Rheumatology (Oxford) 47:8–12.

Hitchon CA, El-Gabalawy HS. 2004. Oxidation in rheumatoid arthritis. Arthritis Res Ther 6:265–278.

Hueber AJ, Asquith DL, Mclnnes IB, Miller AM. 2010. Embracing novel cytokines in RA – complexity grows as does opportunity! Best Pract Res Clin Rheumatol 24:479–487.

Hutas G, Bajnok E, Gal I, Finnegan A, Glant TT, Mikecz K. 2008. CD44-specific antibody treatment and CD44 deficiency exert distinct effects on leukocytes recruitment in experimental arthritis. Blood 112:4999–5006.

Jackson DG. 2009. Immunological functions of hyaluronan and its receptors in the lymphatics. Immunol Rev 230:216–231.

Lee HG, Cowman MK. 1994. An agarose gel electrophoretic method for analysis of hyaluronan molecular weight distribution. Anal Biochem 219: 278–287.

Loniewski KJ, Patial S, Parameswaran N. 2007. Sensitivity of TLR4- and -7-induced NF kappa B1 p105-TPL2-ERK pathway to TNF-receptor-associated-factor-6 revealed by RNAi in mouse macrophages. Mol Immunol 44:3715–3723.

Monzon ME, Fregien N, Schmid N, Falcon NS, Campos M, Casalino-Matsuda SM, Forteza RM. 2010. Reactive oxigen species and hyaluronidase 2 regulate airway epithelial hyaluronan fragmentation. J Biol Chem 285:26126–26134.

Murphy G, Nagase H. 2008. Reappraising metalloproteinases in rheumatoid arthritis and osteoarthritis: Destruction or repair? Nat Clin Pract Rheumatol 4:128–135.

Nagy G, Koncz A, Telarico T, Fernandez D, Ersek B, Buzas E, Perl A. 2010. Central role of nitric oxide in the pathogenesis of rheumatoid arthritis and systemic lupus erythematosus. Arthritis Res Ther 12:210.

Sloane JA, Blitz D, Margolin Z, Vartanian T. 2010. A clear and present danger: Endogenous ligand of Toll-like receptors. Neuromolecular Med 12:149–163.

Stern R, Asari AA, Sugahara KN. 2006. Hyaluronan fragments: An information-rich system. Eur J Cell Biol 85:699–715.

Stern R. 2008. Hyaluronidases in cancer biology. Semin Cancer Biol 18:275–280.

Taylor KR, Yamasaki K, Radek KA, Di Nardo A, Goodarzi H, Golenbock D, Beutler B, Gallo RL. 2007. Recognition of hyaluronan released in sterile injury involves a unique receptor complex dependent on toll-like receptor 4, CD44, and MD-2. J Biol Chem 282:18265–18275.

Takaishi H, Kimura T, Dalai S, Okada Y, D'Armiento J. 2008. Joint diseases and matrix metalloproteinases: A role for MMP-13. Curr Pharm Biotechnol 9:47–54.

Tammi RH, Kultti A, Kosma VM, Pirinen R, Auvinen P, Tammi MI. 2008. Hyaluronan in human tumors: Pathobiological and prognostic messages from cell-associated and stromal hyaluronan. Semin Cancer Biol 18:288–295.

Tanimoto K, Kitamura R, Tanne Y, Kamiya T, Kunimatsu R, Yoshioka M, Tanaka N, Tanaka E, Tanne K. 2010. Modulation of hyaluronan catabolism in chondrocytes by mechanical stimuli. J Biomed Mat Res A 93:373–380.

Veiseh M, Turley EA. 2011. Hyaluronan metabolism in remodelling extracellular matrix: Probes for imaging and therapy of breast cancer. Integr Biol (Camb) 3:304–315.

Wooley PH, Whalen JD, Chapdelaine JM. 1989. Collagen-induced arthritis in mice. VI. Synovial cells from collagen arthritic mice activate autologous lymphocytes in vitro. Cell Immunol 124:227–238.